Available online at www.sciencedirect.com
ScienceDirect
International Journal of Heat and Mass Transfer 50 (2007) 3820–3831
International Journal of HEAT and MASS TRANSFER
www.elsevier.com/locate/ijhmt

Determination of temperature wall functions for high Rayleigh number flows using asymptotics: A systematic approach

C. Balaji [a,*], M. Hölling [b], H. Herwig [b]

[a] Department of Mechanical Engineering, Indian Institute of Technology Madras, Chennai 600 036, India
[b] Institute of Thermo-Fluid Dynamics, Hamburg University of Technology, Denickestrasse 17, D-21073 Hamburg, Germany

Received 31 March 2006; received in revised form 22 January 2007
Available online 16 April 2007

Abstract

This paper presents a systematic approach to determine temperature wall functions for high Rayleigh number flows using asymptotics. An asymptotic analysis of the flow and heat transfer in the near wall region forms the basis for the development of the wall functions. Appropriate normalization of the variables followed by asymptotic matching of the temperature gradients of the inner and outer layers in the overlap region leads to a logarithmic temperature profile as a wall function that has undetermined constants. A key classification that has been made in the present study is the introduction of (1) *The direct problem* and (2) *The inverse problem*. The former means that temperature profiles, either from experiments or Direct Numerical Simulations (DNS), are available and the wall function problem finally reduces to one of determining certain constants in a general wall function formula. More radical and of more interest, is the inverse problem. The idea behind this it is that when a temperature profile can be recast into a Nusselt–Rayleigh correlation, it should be perfectly possible for one to start from a Nusselt–Rayleigh correlation and end up with a wall function for temperature. This approach again will have undetermined constants that can be calibrated from either experimental or DNS data. The main advantage of using the inverse problem is the dispensation of the need to measure temperatures accurately within the boundary layer. For both the direct and inverse problems, a graded treatment to determine the constants is presented. The treatment at its highest level will result in a parameter estimation problem that can be posed as an optimization problem. The optimization problem is then solved by state of the art techniques like Levenberg–Marquardt algorithm and Genetic algorithms (GA) and the solutions are compared. While for the direct problem, the approach is illustrated for the infinite channel problem (a simple flow), for the inverse problem, the approach is elucidated for the Rayleigh–Bénard problem (a complex flow). Finally, a blending procedure to arrive at a universal temperature profile that is valid in the viscous sublayer, buffer and the overlap layers is suggested. The key ideas of (1) using optimization techniques for determining the constants in the wall function and (2) obtaining wall functions from the Nusselt numbers by the inverse approach are expected to be useful for a wide class of problems involving natural convection.

Keywords: Turbulent natural convection; Wall function; Asymptotics; Nusselt–Rayleigh correlation

1. Introduction

Numerical solutions of turbulent flows, with and without heat transfer, are required for many problems of practical interest. These flows may fall under the category of natural, mixed or forced convection. Most CFD software employs algebraic wall function formulations that have been developed, mostly, for forced convection flows, to take care of the effects of the thin layer close to the wall, in order to save computational time and effort. Otherwise, the near wall mesh has to be extremely fine to resolve this sublayer. Models that resolve the sublayer are known as low Reynolds number models. On the other hand, models that do not require resolution of the sublayer due to the incorporation of wall functions are known as high Reynolds number models or simply "standard" models. These

* Corresponding author. Tel.: +91 22574689; fax: +91 22570509.
E-mail address: balaji@iitm.ac.in (C. Balaji).

0017-9310/$ - see front matter © 2007 Elsevier Ltd. All rights reserved.
doi:10.1016/j.ijheatmasstransfer.2007.02.013

Nomenclature

a, b, e, f, g, h	constants in the wall function
C	constant of the overlap temperature profile (Eq. (21))
D	constant of the overlap temperature profile (Eq. (21))
C_∞	asymptotic value of C
D_∞	asymptotic value of D
g	acceleration due to gravity, 9.81 m/s^2
g_i	residue, defined in Eq. (51)
h	spacing of the vertical channel, m
H	characteristic dimension, m
J	Jacobian
Nu	Nusselt number
p	parameter vector (Eq. (52))
q	correction to the parameter vector (Eq. (52))
q_{mol}	conduction heat flux, defined in Eq. (9), W/m^2
q_{turb}	turbulent heat flux, defined in Eq. (9), W/m^2
q_{w}	wall heat flux, defined in Eq. (10), W/m^2
Ra_{T}	turbulent Rayleigh number, $\frac{g\beta T_c H^3}{\alpha\nu}$
Ra	Rayleigh number, $g\beta\Delta\overline{T}H^3/\nu\alpha$
S	residual in Eq. (31)
T_{c}	characteristic temperature, defined in Eq. (6)
T_{C}	cold wall temperature, K
T_{H}	hot wall temperature, K
T_0	reference temperature, K
$\overline{T}$	time averaged temperature at any point, K
T'	fluctuating component of temperature, K
$\overline{u}$	time averaged vertical velocity, m/s
u'	fluctuating component of vertical velocity, m/s
$\overline{v}$	time averaged horizontal velocity, m/s
v'	fluctuating component of horizontal velocity, m/s
x	vertical co-ordinate, m
y	horizontal co-ordinate, m
$y^\times$	dimensionless wall co-ordinate for the inner layer, defined in Eq. (17)
$\hat{y}$	intermediate dimensionless length scale, $y/(H^{1-\gamma}\delta^\gamma)$

Greek symbols

α	thermal diffusivity, m^2/s
β	volumetric expansion coefficient, 1/K
γ	index used in the definition of $\hat{y}$
δ	inner layer thickness, defined in Eq. (17)
$\Delta\overline{T}$	temperature difference, T_{H}–T_{C}, K
ε	dimensionless Rayleigh number, $(Ra/(Ra+10^9))^{0.1}$
η	dimensionless wall distance, defined in Eq. (13)
$\Theta^\times$	dimensionless near wall temperature, defined in Eq. (7)
λ	damping function
ν	kinematic viscosity, m^2/s
Π_1, Π_2	dimensionless groups, defined in Eqs. (5) and (16), respectively
Π_3	dimensionless group, $(=\eta)$
χ	dimensionless Rayleigh number, $Ra/10^{10}$
ξ	dimensionless Rayleigh number, $Ra/10^6$

models do not require fine grids near the wall and hence are computationally efficient. Even so, there are attendant problems in situations where one encounters adverse pressure gradients, buoyancy effects or massive suction/blowing.

In the "standard" models, the governing equations are not solved in the near wall region and these regions are bridged by "universal" near wall velocity and temperature profiles, known as "wall functions". Many of these schemes are semi-empirical (see for example Patankar and Spalding [1], Wolfstein [2], Chieng and Launder [3]) and can only be applied to a limited class of problems. Furthermore, the performance of the wall functions often worsens dramatically if the first grid point is either too close to the wall i.e. it lies within the sublayer or is too far away. Sometimes wall functions are used "recklessly" and this has been poignantly brought out in the work of Craft et al. [4] where the authors state the following "...It was seen as intolerable that successive generations of CFD users should be forced to adopt wholly inadequate wall function formulae as the only alternative to a fine grid analysis...". Craft et al. [5] proposed improved wall functions by adopting a low Reynolds number model of turbulence followed by one dimensional integration. Craft et al. [4] used a simple analytical approach to develop new wall functions. They demonstrated the efficiency of the new wall functions to a few representative problems that included mixed convection in a vertical pipe, a "buoyancy affected" flow. Utyuzhnikov [6] developed wall functions for simulating turbulent flows by employing a method that allows the transfer of boundary condition from a wall to some intermediate point.

Analyzing different approaches shows that the wall functions, in general, have a "forced convection bias". For example, one does not have a "high Rayleigh number model" for a pure natural convection problem. Satisfactory wall treatments for natural convection are very few. Of the very few studies, well known is the work of George and Capp [7] that used asymptotic arguments and obtained a power law for both the velocity and temperature profiles in the near wall region for turbulent natural convection flow over a vertical flat plate. However, because of inadequate data available at that time, these wall functions were not extensively tested. Versteegh and Neuwstadt [8] and Henkes and Hoogendoorn [9] tested these wall functions, several years after they were developed and found that the agreement with experimental data was not very satisfactory. The work of Craft et al. [4] also is for a "buoyancy

affected" flow and one does not know whether it can be extended to the case of pure natural convection.

In consideration of the above reasons, we started out with a goal of developing "exclusive" wall functions for natural convection flows (with possible future extension to mixed convection flows). This is based on an asymptotic analysis of the near wall region with a procedure mirroring what is normally done for deriving the logarithmic law of the wall for forced convection. The end result is, in fact, a logarithmic law of the wall for the temperature in the near wall region and a more complex form for the velocity profile that also includes logarithmic terms. The new wall functions were subsequently tested extensively against available DNS/experimental data. The results for vertical surfaces are documented in Hölling and Herwig [10,11] for Rayleigh—Bénard convection. In this paper, we take this quest for a natural convection wall function to its logical end by looking at the multifarious options and strategies involved in getting the final form of the wall functions along with the constants.

The process leads us to a special classification of the wall function determination problem into two broad heads (1) the direct problem, where the temperature and/or velocity profiles are known and with these, the constants have to be determined and (2) the inverse problem, where we invert a Nusselt–Rayleigh correlation into a temperature wall function and then look at the various methods to determine the constants. The determination of the constants is done in a graded fashion starting from a simple "visual" or least squares fit of the near wall profiles (2 constants) to a sophisticated approach of determining the constants (4 constants now) using parameter estimation techniques. In using the latter approach, the functional forms of the variation of the constants with the Rayleigh number (Ra), consequent upon the Ra not being asymptotically high enough, are of a form that allows an asymptotic extrapolation to $Ra \to \infty$. Since buoyancy induces the shear, the temperature wall function is more important. Thus, we focus our attention on only the temperature wall function. This, however, does not preclude an extension of the methods that are proposed to be discussed in the ensuing sections to determine velocity wall functions.

2. The analytical temperature wall function

The governing equations for fluid flow and heat transfer in the near wall region of turbulent natural convection flows can be reduced, by a standard scaling analysis, to

$$0 = \frac{\partial}{\partial y}\left(\nu\frac{\partial \overline{u}}{\partial y} - \overline{u'v'}\right) + g\beta(\overline{T} - T_0) \tag{1}$$

$$0 = \frac{\partial}{\partial y}\left(\alpha\frac{\partial \overline{T}}{\partial y} - \overline{v'T'}\right) \Longleftrightarrow \alpha\left.\frac{\partial \overline{T}}{\partial y}\right|_{\mathrm{w}} = \alpha\frac{\partial \overline{T}}{\partial y} - \overline{v'T'} = \text{const} \tag{2}$$

Eq. (1) is the x-momentum (axial momentum) equation and Eq. (2) is the thermal energy equation. The pressure term in the momentum equation has been eliminated using the y momentum equation. The coupling arises due to the presence of a term involving buoyancy, and hence the temperature, in the momentum equation. Also implied in Eq. (1) is the Boussinesq approximation. The zeros appearing on the left hand sides of Eqs. (1) and (2) denote that the leading neglected terms in these equations are the convection terms, whose order is small compared to the terms retained in the equations, so long as one is close to the wall.

From Eq. (2), it can be seen that the heat flux in the near wall region has a molecular and a turbulent part and both together are equal to $\alpha\partial\overline{T}/\partial y|_{\mathrm{w}}$, i.e., the total heat flux is independent of the distance from the wall. Therefore, a characteristic temperature T_{c} should be based on that quantity. This also follows from the Buckingham's Pi theorem, recognizing that

$$\overline{T} = f\left(y, H, \alpha, \nu, g\beta, \left.\frac{\partial \overline{T}}{\partial y}\right|_{\mathrm{w}}\right) \tag{3}$$

Here H is the characteristic length of the problem under investigation. In Eq. (3), α and ν are combined to just one quantity $\alpha\nu$ since for a certain fluid they are linked by a fixed Prandtl number, Pr (see [12] for a discussion on the effect of Prandtl number on temperature wall functions). Eq. (3) has six variables including the temperature and there are three basic dimensions in the problem: Length, time and temperature with units, m, s and K. Hence, there would be $6 - 3 = 3$ dimensionless Π groups.

Choosing $\alpha\nu$, $g\beta$ and $\left.\frac{\partial \overline{T}}{\partial y}\right|_{\mathrm{w}}$ as repeating variables the three groups, we have

$$\Pi_1 = \Pi_1\left(\alpha\nu, g\beta, \left.\frac{\partial \overline{T}}{\partial y}\right|_{\mathrm{w}}, \overline{T}\right) \tag{4}$$

Equating the powers of m, s and K on the left and right hand sides leads to

$$\Pi_1 = \frac{\overline{T}}{\left(\frac{\alpha\nu}{g\beta}\left|\frac{\partial \overline{T}}{\partial y}\right|^3_{\mathrm{w}}\right)^{1/4}} \tag{5}$$

We now recognize that Π_1 is the dimensionless temperature and hence the characteristic temperature T_{c} is given by

$$T_{\mathrm{c}} \equiv \left(\frac{\alpha\nu}{g\beta}\left|\frac{\partial \overline{T}}{\partial y}\right|^3_{\mathrm{w}}\right)^{1/4} \tag{6}$$

With this characteristic temperature, a new dimensionless temperature $\Theta^{\times}$ is introduced as:

$$\Theta^{\times} \equiv \frac{T_{\mathrm{H}} - \overline{T}}{T_{\mathrm{c}}} \tag{7}$$

where T_{H} is the hot plate temperature in the flow under question, be it an infinite channel, cavity flow, Rayleigh–Bénard flow or the flat plate boundary layer.

The energy equation (Eq. (2)) can also be written as

$$\frac{q_{\mathrm{mol}}}{\rho c_p}+\frac{q_{\mathrm{turb}}}{\rho c_p}=\frac{q_{\mathrm{w}}}{\rho c_p} \tag{8}$$

$$\text{where } q_{\mathrm{mol}}=k\left|\frac{\partial\overline{T}}{\partial y}\right| \tag{9}$$

$$q_{\mathrm{turb}}=-\overline{v'T'} \tag{10}$$

$$\text{and}\quad q_{\mathrm{w}}=k\left|\frac{\partial\overline{T}}{\partial y}\right|_{\mathrm{w}} \tag{11}$$

With T_{c} according to (6), $\frac{q_{\mathrm{w}}}{\rho c_p}$ can be rewritten as

$$\frac{q_{\mathrm{w}}}{\rho c_p}=\left(\frac{g\beta\alpha^2T_{\mathrm{c}}^4}{\nu}\right)^{1/3} \tag{12}$$

Eq. (12), thus, gives a scale for the wall heat flux. With H, a scale for the wall distance can be found as

$$\eta\equiv\frac{y}{H} \tag{13}$$

Employing the scales for $\overline{T}$, q_{w} and y, Eq. (2) can be non-dimensionalized as

$$\frac{1}{\left(\frac{g\beta T_{\mathrm{c}}H^3}{\alpha\nu}\right)^{1/3}}\frac{\partial\Theta^{x}}{\partial\eta}+q^{+}_{\mathrm{turb}}=1 \tag{14}$$

The term multiplying the dimensionless temperature gradient in the above equation is recognized as $Ra_{\mathrm{T}}^{-1/3}$ where Ra_{T} can be termed as the turbulent Rayleigh number analogous to the turbulent Reynolds number (Re_{T}) defined for turbulent forced convection flows. Since our focus is on high Rayleigh number flows, in the limit of $Ra_{\mathrm{T}}\to\infty$, $q^{+}_{\mathrm{turb}}=1$. This is valid everywhere in the flow except in the region very close to the wall where $q^{+}_{\mathrm{turb}}=0$. *Hence, for large Rayleigh number flows, the turbulent natural convection flow has a two layer structure*. This is characteristic of singular perturbation problems. The flow consists of a *large outer layer* where the molecular heat flux is negligible compared to the turbulent heat flux and a *thin inner layer* where both the heat fluxes are important (see [12] for a detailed discussion on the two layer structure for forced convection flows). The two layer structure can be seen in Fig. 1.

The inner layer thickness is expected to be very small compared to the length scale H of the problem and hence, should not depend on H. In order to arrive at the inner wall thickness, we again take recourse to the Pi theorem. Introducing the second dimensionless group, Π_2 as

$$\Pi_2=\Pi_2\left(\alpha\nu,g\beta,\left|\frac{\partial\overline{T}}{\partial y}\right|_{\mathrm{w}},y\right) \tag{15}$$

and by employing a procedure similar to the one that was used for determining Π_1, we obtain Π_2 as

$$\Pi_2=\frac{y}{\left(\frac{\alpha\nu}{g\beta}\left|\frac{\partial\overline{T}}{\partial y}\right|_{\mathrm{w}}\right)^{1/4}} \tag{16}$$

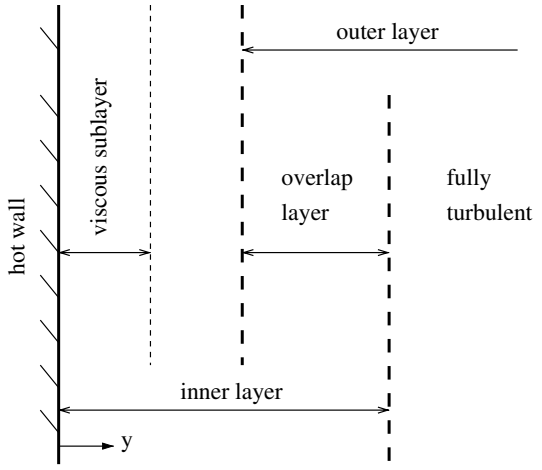

Fig. 1. Two layer structure of the near wall region of high Rayleigh number flows.

The denominator of the right hand side of Eq. (16) can be written as $\left(\frac{\alpha\nu}{g\beta}\left|\frac{\partial\overline{T}}{\partial y}\right|_{\mathrm{w}}\right)^{1/4}=T_{\mathrm{c}}\left|\frac{\partial\overline{T}}{\partial y}\right|_{\mathrm{w}}^{-1}$ so that Π_2 becomes the dimensionless wall co-ordinate for the inner layer and we call this as $y^{\times}$. This is given by

$$y^{\times}\equiv\frac{y}{T_{\mathrm{c}}\left|\frac{\partial\overline{T}}{\partial y}\right|_{\mathrm{w}}}=\frac{y}{\delta} \tag{17}$$

With $\delta\to 0$ as $Ra_{\mathrm{T}}\to\infty$. Hence, the inner layer thickness is indeed small (compared to H) and so our assumption, that processes in the inner layer are independent of H, is justified. The third dimensionless group Π_3 turns out to be η.

A third dimensionless wall distance is now introduced that is valid in the overlap layer between the inner and outer layers. This intermediate variable, with y referred to a length scale between H and δ, is $\hat{y}\equiv y/(H^{1-\gamma}\delta^{\gamma})$ with $0\leqslant\gamma\leqslant 1$, i.e. $\eta<\hat{y}<y^{\times}$. Now, the temperature gradient in the overlap layer (in terms of $\hat{y}$) can be rewritten in terms of $y^{\times}$ and η. Then, for $Ra_{\mathrm{T}}\to\infty$ the overlap layer is reached for $y^{\times}\to\infty$ and $\eta\to 0$, respectively. Thus, we get

$$\frac{\partial\Theta^{\times}(y^{\times})}{\partial\hat{y}}=\lim_{y^{\times}\to\infty}\frac{\partial\Theta^{\times}(y^{\times})}{\partial y^{\times}}\frac{\partial y^{\times}}{\partial\hat{y}}=\lim_{y^{\times}\to\infty}\frac{H^{1-\gamma}\delta^{\gamma}}{\delta}\frac{\partial\Theta^{\times}(y^{\times})}{\partial y^{\times}} \tag{18}$$

$$\frac{\partial\Theta^{\times}(\eta)}{\partial\hat{y}}=\lim_{\eta\to 0}\frac{\partial\Theta^{\times}(\eta)}{\partial\eta}\frac{\partial\eta}{\partial\hat{y}}=\lim_{\eta\to 0}\frac{H^{1-\gamma}\delta^{\gamma}}{H}\frac{\partial\Theta^{\times}(\eta)}{\partial\eta} \tag{19}$$

Using Eqs. (13) and (17) and matching the gradients given by Eqs. (18) and (19) in the overlap layer, we have

$$\lim_{y^{\times}\to\infty}y^{\times}\frac{\partial\Theta^{\times}(y^{\times})}{\partial y^{\times}}=\lim_{\eta\to 0}\eta\frac{\partial\Theta^{\times}(\eta)}{\partial\eta} \tag{20}$$

This is fulfilled only if both sides of Eq. (20) are equal to a constant C. This standard kind of matching is also used for forced convection flows (cf. [13]). An integration of the left hand side of Eq. (20) gives

$$\Theta^{\times}=C\ln(y^{\times})+D \tag{21}$$

With an additional "constant" D that in general will be a function of Ra. If the Ra is not asymptotically high enough, C will also be a function of Ra.

Hölling and Herwig [10] used a slightly different characteristic temperature $T_c \equiv \left(\frac{\alpha^2}{g\beta}\left|\frac{\partial \overline{T}}{\partial y}\right|_w^3\right)^{1/4}$ for their wall function. For reasons already discussed, T_c according to Eq. (6) is used here.

George and Capp [7] introduced different scales of the inner and outer layer, which leads to a situation where the matching of the gradients in the over lap layer, leads to a dependence of the dimensionless temperature on $(y^x)^{-4/3}$. This upon integration leads to a 1/3 power law for both the velocity and temperature. However, for fully developed turbulent forced flow in a channel, recent high precision measurements by Zanoun et al. [14], favor the logarithmic law. Moreover, there is a forced convection analogue to the logarithmic law (here too, there is a single scale for temperature). Even so, it needs to be emphasized that while DNS/experimental velocity and temperature data can always be fitted to a power law, though not necessarily a 1/3 power, this will at best be a "brute force" fit. Continuing these arguments further, even for the forced convection law of the wall, the 1/7 power law is an "empirical best fit" to data that was available at that time and cannot be derived from asymptotic arguments. While this leads to simpler representations for transfer coefficients like the skin friction coefficient and Stanton number, the fact remains that a power law (at least for forced flows) is empirical. So, there is no reason to assume or believe right away that for turbulent natural convection a 1/3 power law exists because one wants an "easy to use" correlation for Nusselt number in the form, $Nu = aRa^{1/3}$ in the end.

A viscous sublayer exists very close to the wall as part of the wall layer, as seen in Fig. 1. Here, the turbulent heat flux is completely damped by the presence of the wall $(-\overline{v'T'} = 0)$. In view of this, the energy equation (Eq. (2)) reduces to

$$\frac{\partial T}{\partial y} = \left|\frac{\partial \overline{T}}{\partial y}\right|_w \tag{22}$$

Eq. (22) can be integrated and we obtain the dimensionless temperature profile as

$$\Theta^\times = y^\times \tag{23}$$

3. Determination of the constants – The direct problem

In the preceding section, a universal temperature profile for the overlap layer was derived based on an asymptotic analysis of the near wall region. This can be used as a wall function in CFD codes. However, the constants in Eq. (21) are, as yet, undetermined. The direct problem referred to above, is the problem of determination of the constants C and D, once we have $\Theta^\times$ vs $y^\times$ from experimental or DNS studies. At this juncture, it is instructive to mention that (1) in general C and D are functions of Ra (based on the actual temperature difference $\Delta\overline{T}$) and hence their determination is not trivial and (2) considerable effort goes into conversion of $\overline{T}$ vs y into $\Theta^\times$ vs $y^\times$. In what follows, a graded approach to determine the constants is presented.

3.1. Level 1 treatment

This is the simplest method to determine the constants, wherein an effect of Ra on the constants is ignored. In order to demonstrate the method(s), a representative problem needs to be chosen. For the direct problem, we choose the problem of turbulent natural convection from a differentially heated vertical channel (see Fig. 2). This geometry has been reasonably well studied and both DNS and experimental results are available. For purposes of determining the constants, we choose the study of Versteegh and Nieuwstadt [8]. In this work, investigations have been carried out for four values of Ra (based on spacing h) namely 5.4×10^5, 8.2×10^5, 2×10^6 and 5×10^6. The temperature versus y data was converted to $\Theta^\times$ vs $y^\times$ and these are plotted on a semi-log plot, as seen in Fig. 3. It is seen that the data show some spread, thereby implicitly suggesting that C and D have to be functions of Ra. Even so, in the level 1 treatment, this effect is ignored and using a "visual best" or a more scientific least square best fit, $C = 0.513$ and $D = 1.81$. The spread of the data around this line is clearly seen in Fig. 3.

3.2. Level 2 treatment

Here, we recognize that C and D are functions of Ra. We assume the following functional forms for C and D

$$C = a + b/\xi \tag{24}$$

$$\text{and} \quad D = e + f/\xi \quad \text{where } \xi = Ra/10^6 \tag{25}$$

Basically, the introduction of ξ is done to ensure that some terms in the temperature wall function expression do not

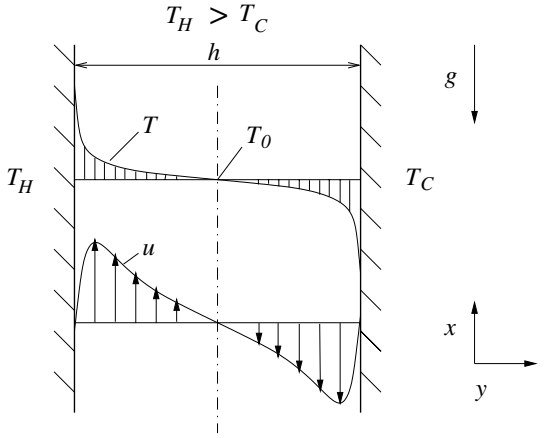

Fig. 2. Turbulent natural convection from an infinite channel.

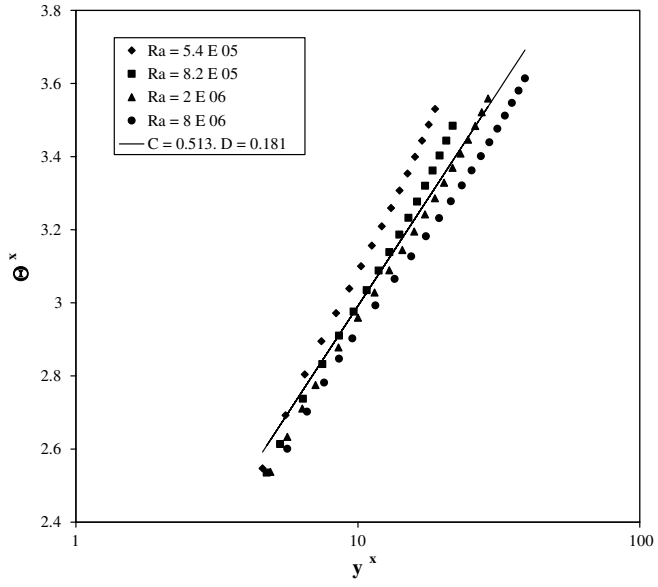

Fig. 3. Determination of the constants in the wall function using level 1 treatment for the direct problem.

become too large if Ra is directly used. A normalized Ra will be smaller and will help us avoid numerical inaccuracies and instabilities in the parameter estimation process. Substituting for C and D in the generic form of the overlap temperature profile (Eq. (21)) leads to

$$\Theta^x = (a\ln(y^\times) + e) + (1/(\xi)(b\ln(y^\times) + f)) \tag{26}$$

It is clear that when $Ra \to \infty$, $1/\xi \to 0$ and so

$$\Theta^\times = a\ln(y^\times) + e \tag{27}$$

Hence, a and e will be the asymptotic constants for the wall function. The first two terms on the right hand side of Eq. (26) constitute the asymptotic part of the temperature profile and the last two terms constitute the Rayleigh number dependent part. Determination of a, b, e and f can be done by a "visual best" method. Here, $\Theta^\times$ vs $y^\times$ are plotted for various values of Ra and the constants C and D are first evaluated for every value of Ra and then their functional forms given in Eqs. (24) and (25) are made use of. Alternatively, this can be done using a least square best fit for every Ra, followed by the procedure discussed above. We now look at the least square best fit method for the data of [8]. The values of C and D for the various values of Ra are given in Table 1. Using the values from this table in Eq. (26), we obtain the final from of the temperature wall function as:

Table 1
Direct problem – level 2 treatment for the infinite channel problem

S. No.	Rayleigh number, Ra	C	D	$1/\xi$
1	5.4×10^5	0.677	1.527	1.852
2	8.2×10^5	0.604	1.604	1.219
3	2×10^6	0.5514	1.681	0.5
4	5×10^6	0.500	1.758	0.2

$$\Theta^x = (0.488\ln(y^\times) + 1.767) + (1/\xi)(0.1009\ln(y^\times) - 0.1324) \tag{28}$$

The asymptotic values of C and D for $\xi \to \infty$, i.e. C_∞ and D_∞ are 0.488 and 1.767, respectively.

The "visual best" approach, for the data of Versteegh and Nieuwstadt [8], is discussed in [10] and the constants a and e, as reported in [10] for a fluid with $Pr = 0.7$ (slightly different from the values reported in the paper because of a different definition of T_c are 0.465 and 2.06, respectively and there is concordance in the values).

Hence, the truly asymptotic temperature profile for the overlap layer is given by

$$\Theta^\times = 0.488y^\times + 1.77 \tag{29}$$

It can be seen that the level 2 treatment gives values of the constants that are different from those obtained from the level 1 treatment, thereby confirming the effect of Ra on the constants which is a consequence of the Rayleigh numbers not being "asymptotically high enough". A parity plot of $\Theta^\times$ (data) and $\Theta^\times$ (pred) with level 1 and 2 treatment can be seen in Fig. 4. It is clear that the level 2 treatment is markedly superior to the level 1 treatment, as expected.

3.3. Level 3 treatment

The general form of the overlap temperature profile with the Rayleigh number dependence built in, as given in Eq. (26) is

$$\Theta^x = (a\ln(y^\times) + e) + (1/\xi)(b\ln(y^\times) + f) \tag{30}$$

A manual evaluation of the constants a, b, e and f, as was done in the level 2 treatment, whether with a visual or a least squares best fit, will become tedious if the data are

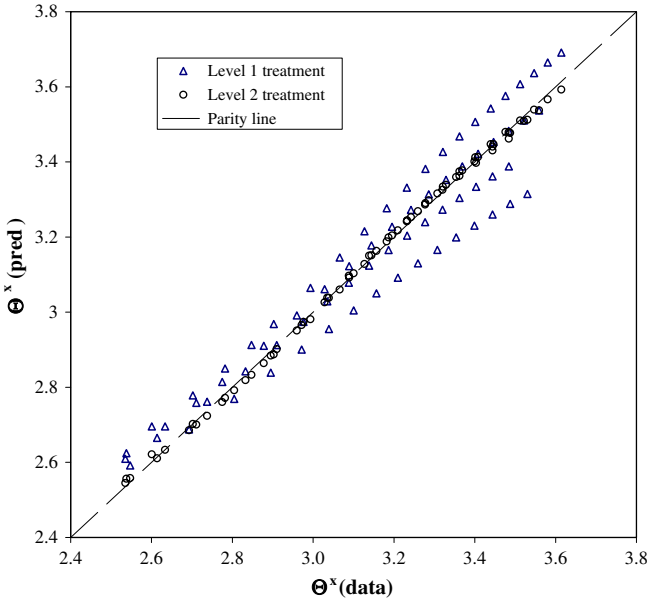

Fig. 4. Parity plot showing agreement of Θ^x (data) with Θ^x (pred) from a level 2 treatment. Also, shown is Θ^x (pred) with level 1 treatment.

available for several values of Ra and hence it would be beneficial, if one can retrieve all the constants simultaneously, once Θ^x vs y^x is available.

For doing the above, one needs to employ a parameter estimation technique that will basically involve the minimization of a residual or cost function S. This can be defined as

$$S = \sum_{i=1}^{n} \left[\Theta_i^x(\text{data}) - \left\{ (a \ln y_i^x + e) + \frac{1}{\xi_i}(b \ln y_i^x + f) \right\} \right]^2 \tag{31}$$

The constants can be determined by a minimization of S once we have $(\Theta_i^x,\ y_i^x)$, ξ_i for all i. Several techniques are available to determine the constants. In this paper, we restrict our attention to the Levenberg–Marquardt algorithm (LMA) and as a consistency check, one set of results are also obtained by using Genetic Algorithms (GA) for purposes of comparison.

3.3.1. Level 3 treatment with the Levenberg–Marquardt algorithm (LMA)

The Levenberg–Marquardt algorithm provides a numerical solution to the mathematical problem of minimizing a sum of squares of several, general, non-linear functions that depend on a common set of parameters like Eq. (31), for example. The algorithm was first developed by Levenberg [15] and later rediscovered by Marquardt [16]. It continues to be the mainstay of many in house codes and most software packages that are currently available for non-linear parameter estimation. Details of the algorithm are provided in Appendix A.

For the problem under consideration, the commercially available DATAFIT 8.1 [17] that works on LMA with double precision was used. With the same data, as was used for level 1 and level 2 treatments, the parameters a, b, e and f were determined and the overlap temperature profile is

$$\Theta^x = (0.487 \ln(y^\times) + 1.77) + (1/\xi)(0.101 \ln(y^\times) - 0.1328) \tag{32}$$

Eq. (32) has a very high correlation coefficient of 99%, which is to be expected in correlations based on numerical data. We will return to this point when we consider the level 3 treatment for the inverse problem with experimental data. The asymptotic constants, which are actually of more interest to us, are 0.487 and 1.77, respectively and these are very close to those obtained by the level 2 treatment (0.488 and 1.767), thus obviating the need to present another parity plot.

In order to have more confidence in the LMA solutions, a set of calculations was also done using another optimization technique namely, Genetic Algorithms (GA). GA is a multi-dimensional search technique that mimics the process of evolution. It starts with an initial set of possible solutions and using the principles of natural selection improves upon these solutions. Every solution is replaced by its binary equivalent of 0 and 1 and the better ones are chosen to "reproduce", followed by a random, crossover of bits from one solution to another. As a safeguard, a low value of mutation (1/20) is generally used, i.e. arbitrarily a 0 is changed into 1 and vice versa, thus mirroring the process of mutation in biology. Recently, GA is being increasingly applied to problems of optimization in heat transfer (see for example [18]). For the problem under consideration, a freely available GA code [19] was used with the following specifications:

Population size : 32 (refers to number of data)
Number of parameters : 4
Probability of crossover : 0.5
Number of generations : 300 (refers to number of iterations)

For the same data set that was used for the LMA, the following results were obtained:

$$\Theta^x = (0.488 \ln(y^\times) + 1.77) + (1/\xi)(0.101 \ln(y^\times) - 0.1328) \tag{33}$$

The above results confirm that the optimization procedure (LMA) adopted in this study for the determination of wall functions is adequate. One can also use other techniques like Artificial Neural Networks (ANN) and Bayesian inference that are known to work well for non-linear parameter estimation. The choice of the technique may become more important if data are available for several values of Ra and/or there is lot of scatter in the data (to be expected in experimental investigations).

3.4. Blending of the temperature profiles

From the available DNS or experimental data for the temperature field (and also the velocity field) in the near wall region, it is clear that while the linear temperature profile $\Theta^\times = y^\times$ holds good for $y^\times \leqslant 1$, the logarithmic profile holds for $y^\times \geqslant 5$. Hence, in the region $1 \leqslant y^\times \leqslant 5$ that is usually known as the buffer layer, the temperature profile changes from linear to logarithmic. The temperature profiles in the sublayer and the overlap layer can be blended, using a procedure outlined in Churchill and Usagi [20], in order to obtain a single, composite expression for the temperature profile that is uniformly valid in the inner, buffer and the overlap layers.

$$\Theta^x_{\text{blended}} = \left(\frac{1}{\Theta^x_{\text{linear}^n}} + \frac{1}{\Theta^x_{\log^n}} \right)^{-1/n} \tag{34}$$

The blending parameter, "n" can be determined by using a non-linear analysis. Employing DATAFIT 8.1 with the LMA and using the DNS data of [8] at the highest Rayleigh number, the above expression can be rewritten as

$$\Theta^x_{\text{blended}} = \left(\frac{1}{y^{xn}} + \frac{1}{(0.487 \ln(y)^x + 1.77)^n} \right)^{-1/n} \tag{35}$$

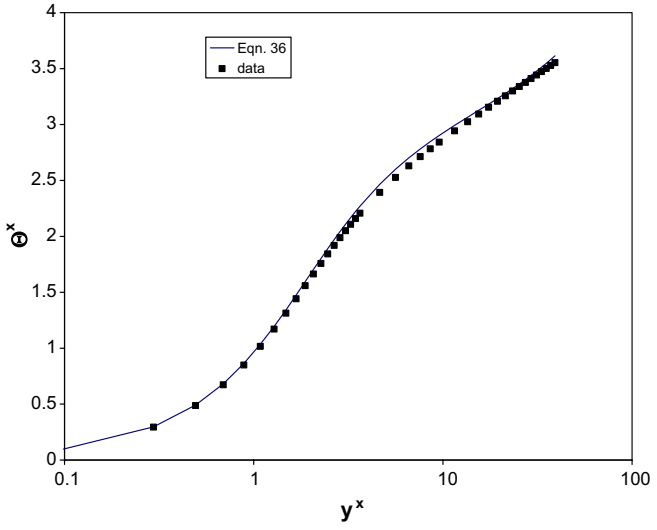

Fig. 5. Temperature data from Versteegh and Nieuwstadt [8] for $Ra = 5 \times 10^6$. Also, shown are Θ^x (blended) as a line.

In the above expression, the constants used are those obtained using the level 3 treatment with LMA. On application of the non-linear parameter estimation (LMA), "n" turns out to be 3.52 ± 0.08. Rounding this off as 3.5, we rewrite the above expression as

$$\Theta^x = \left(\frac{1}{y^{x^{3.5}}} + \frac{1}{(0.487 \ln(y)^x + 1.77)^{3.5}} \right)^{-1/3.5} \tag{36}$$

Eq. (36) is valid for $0 \leqslant y^x \leqslant 200$ and will be particularly useful when employed as a temperature wall function, as it adequately addresses the concern of the CFD analyst who has to otherwise ensure (with the standard wall functions) that the first grid point is not in the buffer layer. The blended profile poses no such restrictions. Fig. 5 shows the excellent agreement between the Θ^x (data) and Θ^x (blended). It is seen that apart from the agreement, the general behavior of Θ^x with $y^\times$ is also adequately captured by the blending procedure. Thus, we just have one equation (Eq. (36)) for the near wall temperature profile that is valid all the way from the wall to the outer layer.

4. Determination of wall functions – the inverse problem

We now look at the inverse problem, where we obtain the temperature wall function directly from the Nusselt number (Nu) vs Rayleigh number (Ra) data. In order to do this, first, the generic form of the overlap temperature profile has to be converted into a Nu–Ra correlation. This is best done though an example.

Consider the case of turbulent Rayleigh–Bénard convection between two infinitely wide horizontal plates. The bottom plate is hot and isothermal at T_H and the upper plate is cold and isothermal at T_C. For this case, there is no mean flow. The first step is the assumption that the universal temperature profile is approximately valid up to the middle of the geometry (midplane). The validity of the overlap temperature profile up to the middle is supported by several studies, both experimental and DNS (cf. [10] and [11]).

At this location,

$$\overline{T} = (T_H + T_C)/2 \tag{37}$$

Therefore, the generic form of the overlap temperature profile (Eq. (21)) becomes

$$\frac{\Delta T}{2T_C} = C \ln(H/2\delta) + D \tag{38}$$

In the above equation, $\Delta T = T_H - T_C$.

Substituting for δ from Eq. (17), we have

$$\frac{\Delta T}{2T_C} = C \ln\left(\frac{H}{2T_c} \left| \frac{\partial \overline{T}}{\partial y} \right|_w \right) + D \tag{39}$$

Now we define the Nusselt number, Nu as

$$Nu = \frac{H}{\Delta T} \left| \frac{\partial \overline{T}}{\partial y} \right|_w \tag{40}$$

and the Rayleigh number, Ra as $g\beta\Delta\overline{T}H^3/\nu\alpha$, where H is the height of the cell and β is the cubic expansivity of the medium. Using these definitions, and substituting for T_c from Eq. (6), we get

$$\frac{Ra^{1/4}}{Nu^{3/4}} = \left(\frac{C}{2} \ln\left(\frac{1}{16} RaNu \right) + 2D \right) \tag{41}$$

This on rearrangement gives,

$$Nu = \frac{Ra^{1/3}}{\left(\frac{C}{2} \ln\left(\frac{1}{16} RaNu \right) + 2D \right)^{4/3}} \tag{42}$$

Eq. (42) can be directly used to obtain C and D (and thus the wall function) once we have Nu vs Ra. This is the "inverse problem". In what follows, we present a graded treatment to determine the constants, an approach similar (though not the same) to the one employed for the direct problem.

4.1. Level 1 treatment

This treatment is analogous to the level 1 treatment for the direct problem. For the Rayleigh–Bénard problem, we use the experimental data of Nikolaenko et al. [21]. In this study, high precision measurements were made in cylindrical annuli with diameter to depth ratio ranging from 0.28 to 0.98. In order to avoid non-Boussinesq effects, we choose data that correspond to $\Delta T \leqslant 5\,^\circ C$. This particular study was chosen for two reasons: (1) it is very recent and (2) if the inversion works for this problem, then it should work for all Rayleigh–Bénard flows in plates, (infinite or otherwise), cylinders and so on. The procedure is clearly visible from the high resolution plot (Fig. 6) and the constants turn out to be $C = 0.127$ and $D = 3.294$.

4.2. Level 2 treatment

The level 1 treatment discussed above gives a "first cut" estimate of the constants. Nevertheless, it provides no

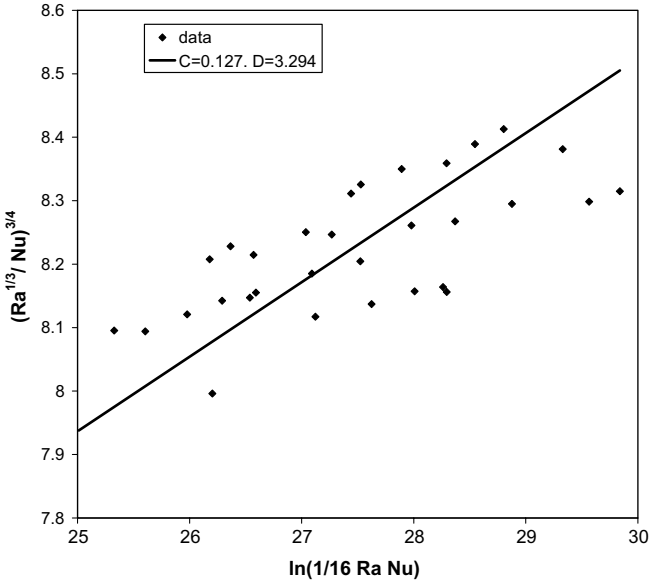

Fig. 6. High resolution plot demonstrating the procedure to determine the constants of the wall function from *Nu* vs *Ra* data for the Rayleigh–Bénard convection problem (level 1 treatment).

information of the variation of the constants with *Ra* and this is crucial if one were to determine the asymptotic values of the constants that are truly independent of *Ra*. In the level 2 treatment, we subdivide the *Ra* range into 2–4 sub-ranges, as deemed fit. For each of this sub-ranges, the constants are evaluated using the procedure similar to the one used for the level 1 treatment (Section 4.1). With this information the constants are asymptotically extrapolated as follows:

$$C = g + h/\chi \tag{43}$$

$$\text{and} \quad D = i + j/\chi \tag{44}$$

where $\chi = Ra/10^{10}$.

The values of C and D thus obtained using the data of [21] are given in Table 2 (since the number of data is limited to 33, the *Ra* range has been subdivided into two sub-ranges).

Using the functional forms of C and D given by Eqs. (43) and (44), respectively and the values seen in Table 2, we have

$$C = 0.1043 + 0.1584/\chi \tag{45}$$

$$\text{and} \quad D = 3.3911 - 1.0479/\chi \tag{46}$$

These are very close to the values of the asymptotic constants $C_\infty = 0.1$ and $D_\infty = 3.43$ determined in an earlier study (cf. [11]). However, in the earlier work, a "visual best" method for C and a least square best method for D was used and this corresponds to the level 2 treatment of the direct problem discussed. Besides Θ^x vs y^x of several investigators (DNS results) were used to arrive at the final values of the constants. The excellent agreement serves to validate one of the key features of this paper: *Nu* vs *Ra* data can be converted to a temperature wall function.

Table 2
Inverse problem – level 2 treatment for the Rayleigh–Bénard convection problem

S. No	Median Rayleigh number, $\overline{Ra}$	C	D	$1/\chi$
1	3.39×10^{10}	0.151	3.082	0.295
2	2.05×10^{11}	0.112	3.340	0.0488

4.3. Level 3 treatment

Here, we need to employ a slightly different strategy for the evaluation of the constants. This is necessitated by the narrow range of the dependent variable of the non-linear estimation, namely $(Ra^{1/3}/Nu)^{3/4}$. Typically, if *Ra* varies by two decades, say $10^9 - 10^{11}$, this parameter for the Rayleigh–Bénard convection problem under question varies from 7.9 to 8.4 (as seen by processing the data of [21]). Hence, while attempting a parameter estimation to retrieve the constants, care must be taken to ensure that C and D are weak functions of *Ra*.

The general form of the *Nu*–*Ra* correlation that is usually reported in literature is the 1/3 or the 2/7 power for *Ra*, multiplied by a constant. This could be thought of as the primary effect. From an asymptotic analysis, we see that this constant, or rather its reciprocal needs to be replaced by a logarithmic term that involves two constants C and D (as discussed earlier) and this is the secondary effect. The final step of assigning functional forms to these constants is to quantify the tertiary effect. In consideration of the above reasons, the following forms are chosen for C and D.

$C = C_\infty \varepsilon$ and $D = D_\infty/\varepsilon$, where $\varepsilon = (Ra/(Ra + 10^9))^{0.1}$. Based on the above, the correlation for *Nu* becomes

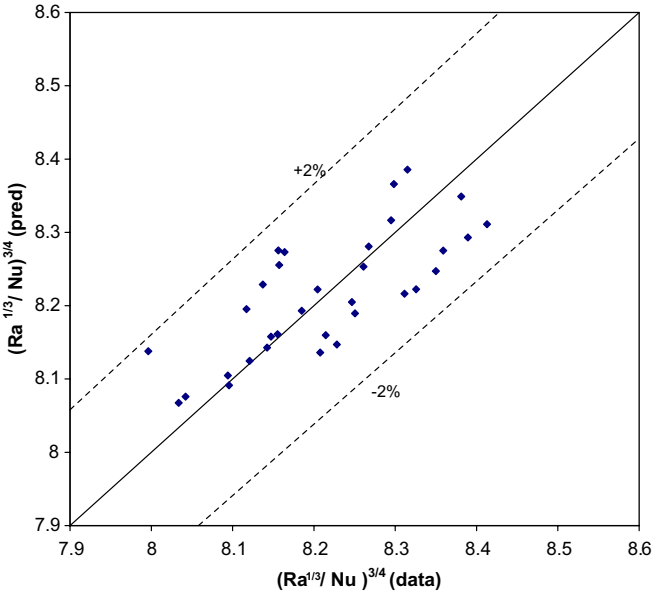

Fig. 7. Parity plot showing agreement of $\left(\frac{Ra^{1/3}}{Nu}\right)^{3/4}$ (data) with $\left(\frac{Ra^{1/3}}{Nu}\right)^{3/4}$ (pred) in the level 3 treatment of the inverse problem.

$$Nu = \frac{Ra^{1/3}}{\left(\frac{C_\infty \varepsilon}{2} \ln\left(\frac{1}{16} RaNu\right) + 2D_\infty/\varepsilon\right)^{4/3}} \tag{47}$$

This is rewritten as

$$\left(\frac{Ra^{1/3}}{Nu}\right)^{3/4} = \left(\frac{C_\infty \varepsilon}{2} \ln\left(\frac{1}{16} RaNu\right) + 2D_\infty/\varepsilon\right) \tag{48}$$

The above is treated as a parameter estimation problem in two independent variables $\ln\left(\frac{1}{16} RaNu\right)$ and ε. The dependent variable is the term seen in the left hand side of Eq. (48). The parameters to be determined are C_∞ and D_∞. Using the procedure outlined in Section 3.3 (with the Levenberg–Marquardt algorithm) with the experimental data of [21], $C_\infty = 0.105$ and $D_\infty = 3.40$. The correlation coefficient is somewhat low at 76%. This, however, is to be expected in view of the scatter in the experimental data. Even so, $\left(\frac{Ra^{1/3}}{Nu}\right)^{3/4}$ (data) and $\left(\frac{Ra^{1/3}}{Nu}\right)^{3/4}$ (pred) agree to within ±2%. This can be seen in the parity plot shown in Fig. 7.

The above overlap profile, together with a linear temperature profile for the viscous sublayer, can be blended (cf. Section 3.4) to obtain a composite expression for the temperature profile that holds for the sublayer, buffer and overlap layers.

5. Discussion

In the preceding sections, a graded treatment was presented to determine the temperature wall functions for turbulent natural convection flows. The concept of the direct and the inverse problems was introduced and it is seen that, even with *Nu–Ra* data, one can obtain the temperature wall functions. The level 3 treatment, wherein the wall function problem is posed as an optimization problem, will become increasingly useful when DNS and/or experimental results are available for several Rayleigh numbers. The most important advantage of this treatment is that accurate measurements of the temperatures within the boundary layer will not be required to obtain wall functions for such flows.

An asymptotic analysis of the near wall velocity field will get us the wall functions for velocity in the near wall region (cf. [10] which discusses a visual best method). The graded treatment will be applicable here too.

As regards the inverse problem, the conversion of the overlap temperature profile into a *Nu–Ra* correlation is more involved for boundary layer flows and complex flows like natural convection in a square cavity (cf. [22]). Even so, the determination of wall functions for such flows is completely feasible within the asymptotic framework and the real problem is the lack of reliable experimental or DNS data for a benchmark problem, like the square cavity problem. By the same token, determination of velocity wall functions using the inverse problem, may pose difficulties in view of the problems associated with measuring the shear stress accurately in such flows. However, DNS stud-

Table 3
Determination of temperature wall functions for high Rayleigh number flows using asymptotics – a systematic approach

Type of treatment	Direct problem	Inverse problem
Level 1 treatment	*Known*: Temperature profiles – DNS/Exptl. *To find*: C and D (best mean values) *Strategy*: Visual or least squares best fit	*Known*: Nu vs Ra –DNS/Exptl. *To find*: C and D (best mean values) *Strategy*: Conversion of $Nu - Ra$ correlation into a wall function followed by visual or least squares best fit
Level 2 treatment	*Known*: Temperature profiles – DNS/Exptl. *To find*: $C = f(Ra)$ and $D = f(Ra)$ such that C_∞ and D_∞ can be determined with asymptotic extrapolation *Strategy*: Visual or least squares best fit followed by asymptotic extrapolation	*Known*: Nu vs Ra – DNS/Exptl. *To find*: $C = f$ (Ra) and $D = f(Ra)$ such that C_∞ and D_∞ can be determined with asymptotic extrapolation *Strategy*: Divide the Ra range into 3 or 4 regions. Get sets of (C, D) by visual or least squares best fit followed by asymptotic extrapolation
Level 3 treatment	*Known*: Temperature profiles – DNS/Exptl. *To find*: $C = f(Ra)$ and $D = f(Ra)$ such that C_∞ and D_∞ can be determined with asymptotic extrapolation *Strategy*: Pose this as a parameter estimation problem (an optimization problem). Use LMA/GA/ANN/Bayesian inference to get functional forms of C and D such that C_∞ and D_∞ can be determined	*Known*: Nu vs Ra – DNS/Exptl. *To find*: $C = f(Ra)$ and $D = f(Ra)$ such that C_∞ and D_∞ can be determined with asymptotic extrapolation *Strategy*: Pose this as a parameter estimation problem (an optimization problem). Use LMA/GA/ANN/Bayesian inference to get functional forms of C and D such that C_∞ and D_∞ can be determined

Basis: Two layer structure of the temperature field in the near wall region. *General form of the overlap temperature profile*: $\Theta^\times = C \ln(y^\times) + D$.

ies should have no problems in this regard. Furthermore, for complex flows like the turbulent Rayleigh–Bénard convection, as of now, a velocity wall function is hard to find, in view of the obvious difficulties associated with analyzing such flows. Even so, preliminary investigations with a first cut approach of using the wall functions for temperature, developed for this problem using an asymptotic analysis and standard wall functions for velocity seem to give encouraging results for the Rayleigh–Bénard problem (cf. [23]).

A bird's eye view of the various treatments discussed in this paper is presented in Table 3.

6. Conclusions

A rigorous analysis of the temperature field in the near wall region of high Rayleigh number flows leads to a logarithmic law for the overlap temperature profile. The constants in this profile are to be calibrated with available DNS/experimental data. In this study, we classified the wall function problem into (i) the direct problem and (ii) inverse problem. The latter involves the conversion of *Nu* vs *Ra* data into a *Nu–Ra* correlation whose form mimics the temperature wall function. The determination of constants for both the direct and the inverse problems was discussed with three levels of treatment starting from the simplest. The procedure was demonstrated for the problem of turbulent natural convection from an infinite channel for the direct problem and the Rayleigh–Bénard convection for the inverse problem. The concept of blending was introduced to obtain just one expression for the temperature profile that is valid for the sublayer, buffer and overlap layers. The level 3 treatment proposed in this study is contemporary and brings in ideas from optimization into the area of asymptotic analysis. This is expected to be useful in the coming years, when we will, hopefully, have substantial DNS/experimental data for turbulent natural convection flows from several geometries.

Acknowledgements

The first author would like to thank the Alexander Von Humboldt foundation, Germany, for supporting his research stay at the Hamburg University of Technology. The authors would also like to thank Mr. M. Deiveegan, Research scholar, Heat Transfer Laboratory, IIT Madras for the help rendered in running the GA simulations.

Appendix A. Levenberg–Marquardt algorithm (LMA)

In Section 3.3.1, a brief introduction to the above algorithm was given. In what follows, the mathematical details of the algorithm are presented.

Eq. (31) that involves the minimization of the residual between the predicted values of temperature and data can be rewritten as

$$S(p) = \sum_{i=1}^{n} [g_i(p)]^2 \tag{49}$$

where p is the parameter vector given by

$$p^{\mathrm{T}} = (a, b, e, f) \tag{50}$$

and

$$g_i = \left[\Theta^x \text{ (data)} - \left\{ \left(a \ln y_{\mathrm{i}}^x + e\right) + \frac{1}{\xi_{\mathrm{i}}} \left(b \ln y_{\mathrm{i}}^x + f\right) \right\} \right] \tag{51}$$

Like other numerical minimization algorithms, the LMA is an iterative technique. The minimization starts with an initial guess for the parameter vector, p. In every iteration, p is replaced by a new estimate $(p + q)$. This is done as follows:

$$g(p + q) \approx g(p) + Jq \tag{52}$$

where J is a matrix of partial derivatives of $(a \ln y_{\mathrm{i}}^x + e) + \frac{1}{\xi_{\mathrm{i}}}(b \ln y_{\mathrm{i}}^x + f)$ taken with respect to the parameters and is known as the Jacobian. The derivatives in many problems (including the present one) are numerically determined.

We seek a minimum for S and consequently $\nabla \cdot S = 0$. This leads to

$$(J^{\mathrm{T}} J)q = -J^{\mathrm{T}} g \tag{53}$$

"q" can be determined from the above equation by inverting (J^{T} J). The key to the LMA is to use a "damping" in Eq. (53), given by

$$(J^{\mathrm{T}} J + \lambda)q = -J^{\mathrm{T}} g \tag{54}$$

where λ is a non-negative damping factor and can be increased or decreased depending on the reduction in S. The iterations stop when S reduces to a predefined limit (convergence criterion).

References

[1] S.V. Patankar, D.B. Spalding, Heat and Mass Transfer in Boundary Layers, Morgan-Grampian Press, London, 1967.
[2] M. Wolfstein, The velocity and temperature distribution in one-dimensional flow with turbulence augmentation and pressure gradient, Int. J. Heat Mass Transfer 12 (1969) 301–318.
[3] C. Chieng, B.E. Launder, On the calculation of turbulent heat transfer downstream from abrupt pipe expansion, Numer. Heat Transfer 3 (1980) 189–207.
[4] T.J. Craft, S.E. Gant, H. Iacovides, B.E. Launder, Development and application of numerical wall-function strategy for complex near-wall flows, in: Proc. ECCOMAS CFD 2001, Swansea, UK, 2001, pp. 1–20.
[5] T.J. Craft, A.V. Gerasimov, H. Iacovides, B.E. Launder, Progress in the generalization of wall-function treatments, Int. J. Heat Fluid Flow 23 (2002) 148–160.
[6] S.V. Utyuzhnikov, Generalized wall functions and their application for simulation of turbulent flows, Int. J. Numer. Methods Fluids 47 (2005) 1323–1328.
[7] W.K. George, S.P. Capp, A theory for natural convection turbulent boundary layers next to heated vertical surfaces, Int. J. Heat Mass Transfer 22 (1979) 813–826.
[8] T.A.M. Versteegh, F.T.M. Nieuwstadt, A direct numerical simulation of natural convection between two infinite vertical differentially heated walls: scaling laws and wall functions, Int. J. Heat Mass Transfer 42 (1999) 3673–3693, DNS data taken from www.ercoftac.org.

[9] R.A.W.M. Henkes, C.J. Hoogendoorn, Numerical simulation of wall functions for turbulent natural convection boundary layer, Int. J. Heat Mass Transfer 33 (1990) 1087–1097.
[10] M. Hölling, H. Herwig, Asymptotic analysis of the near-wall region of turbulent natural convection flows, J. Fluid Mech. 541 (2005) 383–397.
[11] M. Hölling, H. Herwig, Asymptotic analysis of heat transfer in turbulent Rayleigh–Bénard convection, Int. J. Heat Mass Transfer 49 (2006) 1129–1136.
[12] C.L.V. Jayatilleke, The influence of Prandtl number and surface roughness on the resistance of the laminar sub layer to momentum and heat transfer, Prog. Heat Mass Transfer 1 (1969) 193–329.
[13] H. Schlichting, K. Gersten, Boundary-Layer Theory, Springer, Berlin, 2000.
[14] E.S. Zanoun, F. Durst, H. Nagib, Evaluating the law of the wall in two-dimensional fully developed turbulent channel flows, Phys. Fluids 15 (2003) 3079–3089.
[15] K. Levenberg, A method for the solution of certain problems in least squares, Quart. Appl. Math. 2 (1944) 164–168.
[16] D. Marquardt, An algorithm for least squares estimation of non-linear parameters, SIAM J. Appl. Math. 11 (1963) 431–441.
[17] DATAFIT 8.1 documentation, Oakdale Engineering, Oakdale, USA, 2006.
[18] M. Sasikumar, C. Balaji, Optimization of convective fin systems: a holistic approach, Heat Mass Transfer 39 (2002) 57–68.
[19] D.L. Carrol, Genetic algorithms and optimizing chemical oxygen–iodine layers, in: H.B. Wilson, R.C. Batra, C.W. Bert, A.M.J. Davis, R.A. Schapery, D.S. Stewart, F.F. Swinson (Eds.), Developments in Theoretical and Applied Mechanics, vol. 18, School of Engineering, The University of Alabama, USA, 1996, pp. 411–424.
[20] S.W. Churchill, R. Usagi, A general expression for the correlation of rates of transfer and other phenomena, AIChE J. 18 (1972) 1121–1128.
[21] Alexei Nikolaenko, Eric Brown, Denis Funfschilling, Guenter Ahlers, Heat transport by turbulent Rayleigh–Bénard convection in cylindrical cells with aspect ratio one and less, J. Fluid Mech. 523 (2005) 251–260.
[22] C. Balaji, M. Hölling, H. Herwig, Nusselt number correlations for turbulent natural convection flows using asymptotic analysis of the near wall region, ASME J. Heat Transfer, in press.
[23] M. Hölling, H. Herwig, A new Nusselt–Rayleigh number correlation and wall functions for turbulent Rayleigh–Bénard convection, in: Proc. 13th International Heat Transfer Conference, Sydney, 2006.